Exploring how the fast-slow pace of life continuum and reproductive strategies structure microorganism life history variation

Author names

Josje Romeijn & Isabel M. Smallegange

Orcid Josje Romeijn: 0009-0002-2863-9845

Orcid Isabel M. Smallegange: 0000-0001-6218-7358

Affiliations

Josje Romeijn: Theoretical Biology and Bioinformatics, Department of Biology, Utrecht University, Padualaan 8, 3584 CH Utrecht, The Netherlands

Isabel M. Smallegange: School of Natural & Environmental Sciences, Newcastle University, Newcastle upon Tyne, NE1 7RU, UK

Corresponding author and email address

Isabel M. Smallegange – Isabel.smallegange@newcastle.ac.uk

Keywords

Demography, fast-slow continuum, dynamic energy budget integral projection model, life history trait, population matrix model

Repositories

Supplemental data, R code and MatLab code is available as an Online Appendix at https://doi.org/10.6084/m9.figshare.16831543.v2 [27].

Abstract

Studying life history strategies in microorganisms can help predict their performance when complex microbial communities can be categorised into groups of organisms with similar strategies. Microorganisms are typically classified as copiotroph or oligotroph, but it has been proven difficult to generalise their life history strategies to broad lineages. Here we tested if the fast-slow continuum and reproductive strategy framework of macro-organismal life histories can be applied to microorganisms. We used demographic and energy budget data from 13 microorganisms (bacteria, fungi, a protist and a plant) to examine how generation time, survivorship, growth form, age at maturity, recruitment success, and net reproductive rate structure microbial life histories. We found that 79% of microorganism life-history variation fell along two uncorrelated axes. Like macro-organisms, we found a fast–slow pace of life continuum, including shorter-lived microorganisms at one end, and longer-lived microorganisms that mature later in life at the other. Also, like macro-organisms, we found a second, reproductive strategy axis, with microorganisms with greater lifetime reproductive success and decreased mortality at older age at one end, and microorganisms with the opposite characteristics at the other end. Microorganismal life history strategies did not covary proportionally to their shared evolutionary history. Thus, whereas this work suggests that the macro-organismal fast-slow continuum and reproductive strategy framework could be realistically applied to microorganisms, their life history processes cannot be inferred from patterns in taxonomic composition.

Impact statement

Animals and plants show distinct differences in their pace of life: some have high reproduction and high mortality, others low. Here we show that microorganisms display similar such life history patterns, igniting future research on microbial life history strategies.

Data summary

Supplemental data, R code and MatLab code are deposited in Figshare at https://doi.org/10.6084/m9.figshare.16831543.v2 [27].

Introduction

Different life history strategies capture different combinations of survival, growth and reproduction (demographic) rates of individuals [1] that determine the dynamics of populations. Studying life history strategies in microorganisms can help predict their performance when complex microbial communities can be categorised into organismal groups with similar strategies. Microorganisms are typically classified along a copiotroph-oligotroph dichotomy [2], where copiotrophs grow faster and rely on resource availability, but oligotrophs efficiently exploit resources at the expense of growth rate. In soils, for example, some bacterial phyla are present in greater relative abundance in response to sucrose addition, indicating copiotrophic strategies, whereas other bacterial phyla were either unresponsive or responded negatively, suggesting oligotrophic strategies [3]. Ramin and Allison [4] added a third, maintenance type to the dichotomy. Classifying microorganisms as copiotroph-oligotroph at the phylum level remains prevalent but more ecologically realistic frameworks are needed as bacterial lineages within phyla can have distinct metabolic and ecological roles [5].

In macro-organisms, the majority of life history variation is structured along (i) a fast-slow life history continuum with fast-growing, short-lived species at one end, and slow-growing, long-lived species at the other [6-8], and (ii) a reproductive strategy axis that for higher plants has iteroparous species that reproduce multiple times as adults at one end and semelparous plants that reproduce only once at the other [7,9], whereas for animals this axis is defined by the distribution of age-specific mortality hazards and the spread of reproduction [10]. We do not know if microorganismal life history variation can be structured along these same life history strategy axes [11] and if this would provide a more ecologically realistic life history framework for microbial ecologists. Such a framework could be useful because life history dynamics of individual microbial species influence processes such as human disease progression [12], human-microbe interactions [13] and even ecological strategies of coral species [14].

The aim of this explorative study is to investigate main axes of variation in microorganism life histories to offer an alternative life history framework when studying the performance of microorganisms. To this end, we first adapted a dynamic energy budget integral projection model (DEB-IPM) [15] to the microorganism life cycle. Specifically, the microorganismal DEB-IPM is a discrete-time, structured demographic model that takes data on individual cell life histories as input parameters to describe how individual cells grow according to a von Bertalanffy growth curve [16], and reproduce by binary fission to produce two offspring [17], after which individuals die. We assume that individuals have a constant background mortality. We parameterised DEB-IPMs for 13 microorganisms, including bacteria, fungi, a plant and a protist to calculate seven life history traits that inform on schedules of survival, growth, and reproduction [1]: generation time, survivorship curve, age at maturity, progressive growth (indicating size increase), retrogressive growth (indicating shrinking), mean recruitment success and net reproductive rate. We then evaluated the variation in these traits along major (life history strategy) axes using a phylogenetically corrected principal component analysis (PCA). By measuring if species life history strategies covary proportionally to their shared evolutionary history, we can assess if the fast-slow reproductive strategy framework can be used to support inferences about life history processes from patterns in taxonomic composition of microorganisms (as has been common practice by microbial ecologists [5].

Methods

Brief description of the DEB-IPM

The demographic function that describes growth in the microorganismal DEB-IPM [15] is derived from the Kooijman-Metz model [16], which assumes that individual (micro)organisms are isomorphic (body surface area and volume are proportional to squared and cubed length, respectively). The rate at which an individual (cell) ingests food, *I*, is assumed to be proportional to the maximum ingestion rate I_{max}, the current feeding level *Y* and body surface area, and hence to the squared length of an organism: $I = I_{max}YL^2$. Ingested food is assimilated with a constant efficiency ε. A constant fraction κ of assimilated energy is allocated to respiration (the processes by which a cell obtains the oxygen it needs to produce energy and eliminate waste); this respiration energy equals $\kappa\varepsilon I_{max}YL^2$ and is used to first cover maintenance costs, which are proportional to body volume following ξL^3 (ξ is the proportionality constant relating maintenance energy requirements to cubed length), while the remainder is allocated to somatic growth. This means that, if an individual cell survives from hour *t* to hour *t* + 1, it grows from length *L* to length *L'* following a von Bertalanffy growth curve, $\frac{dL}{dt} = \dot{r}_B(L_m \cdot Y - L)$, where $\dot{r}_B$ is the von Bertalanffy growth rate and $L_m = \kappa\varepsilon I_{max}/\xi$ is the maximum length under conditions of unlimited resource. Both κ and I_{max} are assumed to be constant. However, the role of κ in the DEB-IPM is mostly implicit, as κ is used as input parameter only in the starvation condition (see below), whereas L_m is measured directly from data.

Growth, as described above, as well as survival and reproduction are captured in the DEB-IPM by four fundamental functions to describe the dynamics of a well-mixed population comprising cohorts of individual cells of different sizes [15]: (1) the survival function, $S(L(t))$ (unit: h^{-1}), describing the probability of surviving from hour *t* to hour *t*+1; (2) the growth function, $G(L', L(t))$ (unit: h^{-1}), describing the probability that an individual of body length *L* at hour *t* grows to length *L'* at *t* + 1, conditional on survival; (3) the reproduction function, $R\big(L(t)\big)$ (unit: # h^{-1}), giving the number of offspring produced between hour *t* and *t* + 1 by an individual of length *L* at hour *t*; and (4) the parent-offspring function, $D(L', L(t))$ (unit: h^{-1}), the latter which describes the association between the body length of the parent cell *L* and offspring cell length *L'* (i.e. to what extent does offspring size depend on parental size). Denoting the number of cells at hour *t* by $N(L, t)$ means that the dynamics of the cell length number distribution from hour *t* to *t* + 1 can be written as:

$$N(L', t+1) = \int_{\Omega} \left[D(L', L(t))R\big(L(t)\big) + G(L', L(t))S(L(t))\right]N(L, t)dL \qquad \text{eqn 1}$$

where the closed interval Ω denotes the cell length domain. Note that this simple DEB-IPM does not account for temperature effects or reserve dynamics (which can, however, be an acceptable simplification [18]). Implicitly underlying the population-level model of eqn 1, like in any IPM, is a stochastic, individual-based model, in which individuals follow Markovian growth trajectories that depend on an individual's current state (Easterling et al. 2000). This individual variability is in standard IPMs modelled in the functions describing growth, $G(L', L(t))$, and the parent-offspring association, $D(L', L(t))$, using a probability density distribution, typically Gaussian [19]. In the DEB-IPM, this individual variability arises from how individuals experience the environment; specifically, the experienced feeding level *Y* follows a Gaussian distribution with mean *E*(*Y*) and standard deviation σ(*Y*). It means that individual cells within a cohort of length *L* do not necessarily experience the same feeding level due to demographic stochasticity (e.g. individuals, independently of each other, have good or bad luck in their feeding experience).

The survival function $S(L(t))$ in eqn 1 is the probability that an individual of cell length L survives from hour t to $t + 1$:

$$S(L(t)) = \begin{cases} (1 - p_D)e^{-\mu} & \text{for } L \leq L_m E(Y)/\kappa \\ 0 & \text{otherwise} \end{cases} \qquad \text{eqn 2}$$

assuming a constant background mortality rate μ (h^{-1}). The parameter L_m (μm) is the maximum cell length under conditions of unlimited abundance of food of the highest, relative quality, $E(Y) = 1$. The probability of an individual dividing, and subsequently produce $n_O = 2$ offspring, p_D, enters the survival function to represent binary fission [17], because reproduction in microorganisms entails that the dividing individual ceases to exist. Individuals die from starvation at a cell length at which maintenance requirements exceed the total amount of assimilated energy, which occurs when $L > L_m \cdot E(Y)/\kappa$ and hence, then, $S\big(L(t)\big) = 0$ (e.g., an individual of size L_m will die of starvation if $E(Y) < \kappa$).

The function $G(L', L(t))$ is the probability that an individual of cell length L (μm) at hour t grows to length L' at $t + 1$, conditional on survival, and follows a Gaussian distribution [19]:

$$G(L', L(t)) = \frac{1}{\sqrt{2\pi\sigma_L(L(t+1))}} e^{\frac{-(L' - E(L(t+1))^2}{2\sigma_L^2(L(t+1))}} \qquad \text{eqn 3}$$

with

$$E\big(L(t+1)\big) = L(t)e^{-\dot{r}_B} + \big(1 - e^{-\dot{r}_B}\big)L_m \cdot E(Y), \qquad \text{eqn 4}$$

and

$$\sigma^2(L(t+1)) = (1 - e^{-\dot{r}_B})^2 L_m^2 \sigma^2(Y), \qquad \text{eqn 5}$$

where $\dot{r}_B$ is the von Bertalanffy growth rate and $\sigma(Y)$ is the standard deviation of the expected feeding level, assuming individuals can shrink under starvation conditions.

The reproduction function $R(L(t))$ follows a 'pre-breeding' census as cell division, i.e. reproduction, is fatal. $R(L(t))$ gives the number of offspring produced between hour t and $t + 1$ by an individual of cell length L (μm) at hour t:

$$R(L(t)) = \begin{cases} 0 & \text{for } L_b \leq L < L_d \\ n_O \cdot p_D & \text{for } L_d \leq L \leq L_m E(Y)/\kappa \end{cases} \qquad \text{eqn 6}$$

An individual always divides to produce $n_O = 2$ offspring [one parent and one offspring cell]. We set the cell length at which individuals divide, L_d (μm), equal to the asymptote of the von Bertalanffy growth curve in cell length so that $L_d = E(Y) \cdot L_m$. Only surviving adults reproduce; thus, only individuals within a cohort of cell length $L_d \leq L \leq L_m Y/\kappa$ reproduce. The probability of an individual dividing, p_D, equals:

$$p_D = \begin{cases} 0 & \text{for } L < L_d \\ 1 & \text{for } L \geq L_d \end{cases} \qquad \text{eqn 7}$$

Note that the probability of dividing also enters the survival function as division is fatal.

The probability density function $D(L', L(t))$ gives the probability that the offspring of an individual of cell length L are of length L' at hour $t + 1$:

$$D(L', L(t)) = \begin{cases} 0 & \text{for } L < L_d \\ \frac{1}{\sqrt{2\pi\sigma^2_{L_b}(L(t))}} e^{\frac{-(L' - E_{L_b}(L(t)))^2}{2\sigma^2_{L_b}(L(t))}} & \text{otherwise} \end{cases} \quad \text{eqn 8}$$

Where $E_{L_b}(L(t))$ is the expected cell length of offspring produced by a cohort of individuals with length $L(t)$, and $\sigma^2_{L_b}(L(t))$ the associated variance. For simplicity, we set $E_{L_b}(L(t)) = L_b$ (μm) constant, and assumed its associated variance, $\sigma^2_{L_b}(L(t))$, to be negligibly small so that offspring within a species are evenly sized.

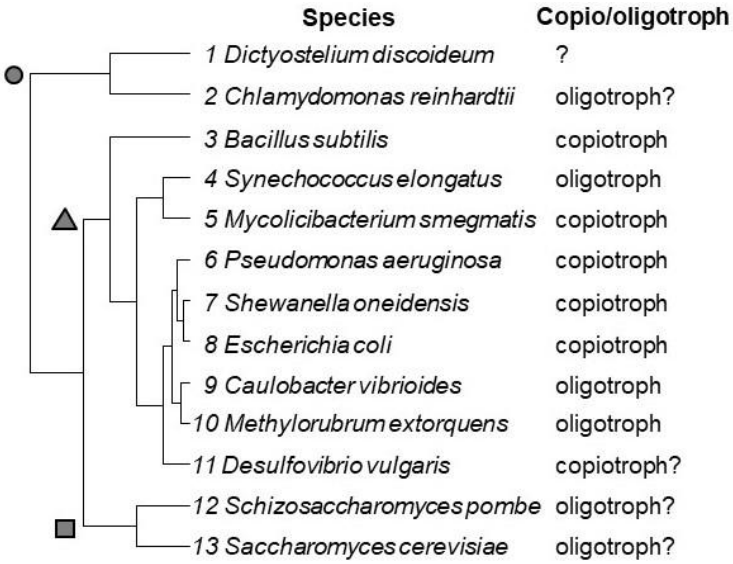

Fig. 1. Phylogenetic tree of the 13 study species created using the *rotl* package [54] to download a tree from the Open Tree of Life (OTL) [55], after taxonomical updating using the R library *taxize* [56] (input names of *Synechococcus elongatus*, *P. aeruginosa* and *Escherichia coli* were changed to *Synechoccocus elongatus* CCMP1630, *Pseudomonas aeruginosa* 148 and *Escherichia coli* 402290, respectively). Branch length was computed using the *compute.brlen* in the R package *ape* [57]. Polytomies were collapsed using the function *multi2di* in *ape* [55]. Copiotroph and oligotroph classification was according to Stone et al. 2023 for species 2-10, and suspected classifications (indicated with questions marks) are from [58] (species 2), [59] (species 11), and [60] (species 12-13).

Parameterization of the DEB-IPM

The projection interval between time t and time $t + 1$ was set at 1 hour; all rates and durations are therefore expressed per hour, or in hours, respectively. We parameterized DEB-IPMs for 13 microorganisms (Fig. 1) (Table 1), with constant values for $\kappa = 0.9$ (for macro-organisms, κ is assumed to be 0.8; we assumed this would be higher for microorganisms as most energy goes into respiration and not reproduction), $\mu = 0.01$ h^{-1} (assuming background mortality under laboratory circumstances is very low), and $n_O = 2$ (as one microorganism divides to produce two offspring) (Table 1). Values of L_b, L_d, L_m, and $\dot{r}_B$ were taken from the literature (references in Table 1) or

Table 1. Model parameters for the 13 microorganisms (Fig. 1). Parameters are expected feeding level $E(Y)$, the fraction of assimilated energy allocated to respiration, κ, cell length at birth, L_b, length at division, L_d, maximum length, L_m, mortality rate, μ, von Bertalanffy growth rate, $\dot{r}_B$, and number of offspring produced, n_O. Units are in brackets. Superscript numbers are references. Species numbers are the same as in the Fig. 1. See further main text.

		Model parameters							
ID	**Species (kingdom)**	**E(Y)** (–)	**κ** (–)	L_b (μm)	L_d (μm)	L_m (μm)	**μ** (h^{-1})	n_O (#)	$\dot{r}_B$ (h^{-1})
1	*Dictyostelium discoideum* (Protista)	0.80	0.90	15.26 [24]	24.74 [24]	48.48 [24]	0.01	2	0.12
2	*Chlamydomonas reinhardtii* (Plants)	1.00	0.90	12.64 [73]	27.26 [73]	29.23 [73]	0.01	2	0.03
3	*Bacillus subtilis* (Bacteria)	0.80	0.90	3.84 [23]	6.89 [23]	13.87 [23]	0.01	2	1.62
4	*Synechococcus elongatus* (Bacteria)	1.00	0.90	2.04 [72]	5.98 [72]	8.031 [72]	0.01	2	0.03
5	*Mycobacterium smegmatis* (Bacteria)	0.80	0.90	5.06 [64]	8.72 [64]	11.96 [65]	0.01	2	0.09
6	*Pseudomonas aeruginosa* (Bacteria)	0.80	0.90	3.86 [22]	17.34 [22]	26.00 [68]	0.01	2	0.25
7	*Shewanella oneidensis* (Bacteria)	0.80	0.90	1.35 [69]	3.35 [69]	5.00 [69]	0.01	2	0.17
8	*Escherichia coli* (Bacteria)	0.50	0.90	2.18 [66]	3.46 [66]	8.00 [67]	0.01	2	5.21
9	*Caulobacter vibrioides* (Bacteria)	0.70	0.90	1.76 [70]	3.22 [70]	5.30 [71]	0.01	2	1.10
10	*Methylorubrum extorquens* (Bacteria)	0.90	0.90	1.71 [74]	4.40 [74]	5.24 [74]	0.01	2	0.15
11	*Desulfovibrio vulgaris* (Bacteria)	1.00	0.90	3.15 [25]	6.18 [25]	6.19 [25]	0.01	2	0.49
12	*Schizosaccharomyces pombe* (Fungi)	0.90	0.90	8.67 [61,79]	16.00 [61,79]	19.43 [62]	0.01	2	0.69
13	*Saccharomyces cerevisiae* (Fungi)	0.99	0.90	3.78 [37]	8.12 [37]	8.24 [20]	0.01	2	0.56

estimated from other data. Specifically, in case of *S. cerevisiae*, we calculated cell length as the cell diameter $2r$ (μm) from cell volume V (μm^3), assuming *S. cerevisiae* cells are sphere-shaped so that $V = \frac{4}{3}\pi r^3$, from which follows that cell length equals $2r = 2\left(\frac{3}{4\pi}V\right)^{1/3}$. To calculate L_m for *S. cerevisiae*, we used the volume of a mother cell and bud [20], and subtracted the volume of the mother cell at division from the volume of the mother cell at birth, assuming that the size at birth of the mother equals the bud's size. Cell length of the mother and bud were calculated from the volume measures as before, and added together to give maximum length, L_m, of *S. cerevisiae*. In case of *Chlamydomonas reinhardtii*, we assumed that, given their shape, cells were proportioned as 4 × 4 × 10 μm [21]. Given the fact that cell volume $V = \frac{4}{3}\pi r^3$ and $r^3 = 4a \cdot 4a \cdot 10a$, gives cell length as $10a = \sqrt[3]{3V/(640\pi)}$, where a is the ratio between the 3 dimensions of the cell, making '10a' the longest cell dimension and therefore interpretable as cell length. In case of *Mycobacterium smegmatis*,

212 measures of cell length at birth and the elongated length of a single cell were combined to give L_m. In
213 case of *Pseudomonas aeruginosa*, only log values of cell length were available [22], which we
214 backtransformed. Cell length measures of *Bacillus subtilis* were available for different media, and we
215 used those values obtained for cells grown on a favourable, glycerol rich medium [23]. In case of
216 *Dictyostelium discoideum*, we inferred from photos that cells are circle-shaped in between birth and
217 mitosis [24], so that cell surface $S = \pi r^2$, from which follows that the cell length equals $2r = 2\sqrt{S/\pi}$.
218 Cell surfaces measures to calculate cell lengths of *D. discoideum* were taken from two timeframe
219 photos taken between mitosis and birth [24] Finally, we manually measured cell lengths of
220 *Desulfovibrio vulgaris* from a series of scale-barred images of cell length over time [25]. For all
221 species, we estimated the von Bertalanffy growth rate, $\dot{r}_B$, using a nonlinear least-squares
222 estimation procedure in R (nls function) [26] to fit the equation $L_t = L_d - [L_d - L_b]e^{-\dot{r}_B t}$ for $\dot{r}_B$
223 [15] against observed growth curves of cell length L_t (µm) over time t (hours), taken from the
224 literature (see R code in [27]).

225 **Identifying life history patterns**

226 For each species, we used their DEB-IPM to calculate in MATLAB [version 9.10.01602886 R2021a]
227 seven representative life history traits: generation time T, the shape of the survivorship curve H, age
228 at maturity L_α, progressive growth γ, retrogressive growth ρ, mean recruitment success φ, and net
229 reproductive rate R_0 [9] (Table 2) that inform on schedules of survival, growth and reproduction.
230 Because all individuals die after reproducing, we did not include mature life expectancy or degree of
231 iteroparity [9]. We set $E(Y)$ for each species such that it mimics favourable laboratory conditions and
232 exponential growth, so that $\lambda > 1$ and $R_0 > 1$ (Table 3). We evaluated the variation in these traits
233 along major axes using phylogenetically corrected principal component analysis (p-PCA) [28]
234 conducted in R [26] to identify the major life history strategy axes. To this end we used the *phyl.pca*
235 function in the R library *phytools* [7,9,28], after log-transforming and scaling values to $\mu = 0$ and SD =
236 1 to agree with PCA assumptions.

237 We estimated Pagel's λ to inform on the phylogenetic correlation between species traits expected
238 under Brownian motion [29], which varies between 0 (phylogenetic independence) and 1 (species
239 traits covary proportionally to their shared evolutionary history). We used Pagel's λ because it has
240 been used successfully in previous cross-taxonomical PCAs on life history traits [7-9], it can describe
241 the evolution of bacterial trait distributions well [30], and suffers from low type I and II errors for
242 phylogenies of varying sizes [31]. Pagel's λ is estimated jointly for all life history traits [28]. Note that
243 Pagel's λ does not detect non-Brownian models of evolution, which can yield phylogenetic
244 dependence ($\lambda = 1$). Intermediate levels of phylogenetic dependence ($0 < \lambda < 1$) could result from
245 the Ornstein-Uhlenbeck mode of evolution (e.g, [32,33]), in which phylogenetic influence decays
246 through time as species trait values move toward an evolutionary optimum irrespective of the
247 starting point [29]. In the simplest, non-Brownian model, traits may evolve instantaneously in
248 response to selection, in which case traits would show no phylogenetic dependence ($\lambda = 0$).
249 Additional tests are required to distinguish these forms of models. Since Pagel's λ was close to 0 (see
250 Results), we also conducted a normal PCA on the life history traits. We assessed the significance of
251 PC axes using Kaiser's criterion [34]).

Table 2. Life history traits and their loadings onto the first two PC axes. To calculate life history traits, we discretised the IPM (Eqn 1) by dividing the length domain Ω into 200 very small-width discrete bins, resulting in a matrix **A** of size $m \times n$, where $m = n = 200$, and which dominant eigenvalue equals λ. Mean lifetime reproductive success R_0 is the dominant eigenvalue of the matrix $\mathbf{F} = \mathbf{V}(\mathbf{I} - \mathbf{GS})^{-1}$, where **I** is the identity matrix and **V** = **DR**, with **D** as the parent-offspring association, **R** the reproduction, **G** the growth and **S** the survival matrix (Caswell 2001); this gives generation time $T = \log(R_0)/\log(\lambda)$ [75]. The mean life expectancy, η_e, is calculated as $\eta_e = \mathbf{1}^{\mathrm{T}}\mathbf{N}$, where **1** is a vector of ones of length m and **N** is the fundamental matrix $\mathbf{N} = (\mathbf{I} - \mathbf{S})^{-1}$. The longevity of an individual of length L is η_L, which means we can calculate age at sexual maturity $L_\alpha = \eta_{L_b}$ and mature life expectancy $L_\varpi = \eta_{L_p}$ so that $\eta_e = L_\alpha + L_\varpi$ [76: eqn 4.21]. l_x is the probability of surviving to age at least x, and m_x is the average fertility of age class x (cf. [77]. $\overline{\mathbf{G}}$ is the mean of **G**, $\overline{\mathbf{V}}$ is the mean of **V,** and i and j are the row and column entries of the matrix, respectively. The vital rates included in the studied set of fundamental life history traits (progressive growth γ, retrogressive growth ρ, and sexual reproduction φ) were averaged across the columns j (the length bins), weighted by the relative contributions of each stage at stationary equilibrium. For example, to calculate mean sexual reproduction φ, we summed the values in the columns j of the **V** matrix and multiplied each φ_{ij} by the corresponding jth element w_j of the stable stage distribution **w**, calculated as the right eigenvector of **A**.

Life history trait	Symbol	Definition	Equation	p-PC1	p-PC2	p-PC3	PC1	PC2	PC3
Generation time	T	Number of hours required for the individuals of a population to be replaced by new ones	$T = \frac{\log(R_0)}{\log(\lambda)}$	**0.98**	-0.02	-0.08	0.48	-0.02	-0.07
Survivorship curve	H	Keyfitz' entropy ($H < 1$ denotes increasing mortality rate with age, $H > 1$ denotes decreasing mortality rate with age, $H = 1$ denotes a constant mortality rate with age) [78].	$H = -\frac{\sum_{x=0}^{x=\eta_e} \log(l_x) l_x}{\sum_{x=0}^{x=\eta_e} l_x}$	0.45	**-0.78**	-0.33	0.22	**-0.70**	-0.31
Age at maturity	L_α	Number of hours for an individual in the population to become reproductive	$L_\alpha = \eta_{L_b}$	**0.98**	-0.06	-0.06	0.48	-0.05	-0.06
Progressive growth	γ	Mean probability of growing to a larger length across the length domain Ω.	$\gamma = \sum_i^m \overline{\mathbf{G}}_{i,j} \overline{\mathbf{w}}_j \vert_{i<j}$	**0.92**	0.24	0.05	0.44	0.21	0.04
Retrogressive growth	ρ	Mean probability of growing to a smaller length across the length domain Ω.	$\rho = \sum_i^m \overline{\mathbf{G}}_{i,j} \overline{\mathbf{w}}_j \vert_{i>j}$	**-0.53**	-0.25	**-0.78**	-0.26	-0.22	**-0.73**
Mean recruitment success	φ	Mean per-capita number of recruits across the length domain Ω.	$\varphi = \sum_i^m \overline{\mathbf{V}}_{i,j} \overline{\mathbf{w}}_j$	**-0.99**	0.04	0.07	-0.48	0.04	0.06
Net reproductive rate	R_0	Mean number of recruits produced during the mean life expectancy of an individual in the population.	$R_0 = \sum_{x=0}^{x=\eta_e} l_x m_x$	-0.16	**-0.72**	**0.65**	-0.08	**-0.65**	**0.60**

Loadings in bold indicate a high contribution (greater than ±0.50) of the life-history trait to the PC axis. p-PC axes are from the phylogenetically constructed PCA, and PC axes from a 'normal' PCA.

Results

The range of microorganismal life history traits was captured by the first three p-PC axes of the p-PCA, which together explained 79% of the variation (Fig. 2A). The life history traits most closely aligned with p-PC1 are related to the fast-slow continuum [1]: generation time (*T*), age at maturity (L_α) and mean recruitment success (φ) had the greatest loadings onto p-PC1. The positive loading of generation time onto p-PC1 had an opposite loading for mean recruitment success, supporting a trade-off between highly reproductive species and population turnover [1] (Table 2). The rate of individual cell growth (progressive growth, γ) and shrinkage (retrogressive growth, ρ) also loaded onto p-PC1 (Table 2). Thus, as we move from negative to positive scores along p-PC1, individuals increase their allocation to individual growth and to the longevity-related life history trait age at maturity and decrease in population turnover (i.e., greater generation time) at the expense of the production of new recruits (Fig. 2A). Only at the extreme ends of this pace of life continuum was there a match between copiotrophs at the fast end and oligotrophs at the slow end of the continuum (red (copiotroph) and blue (oligotroph) convex hulls do not overlap at the extreme ends in Fig. 2A).

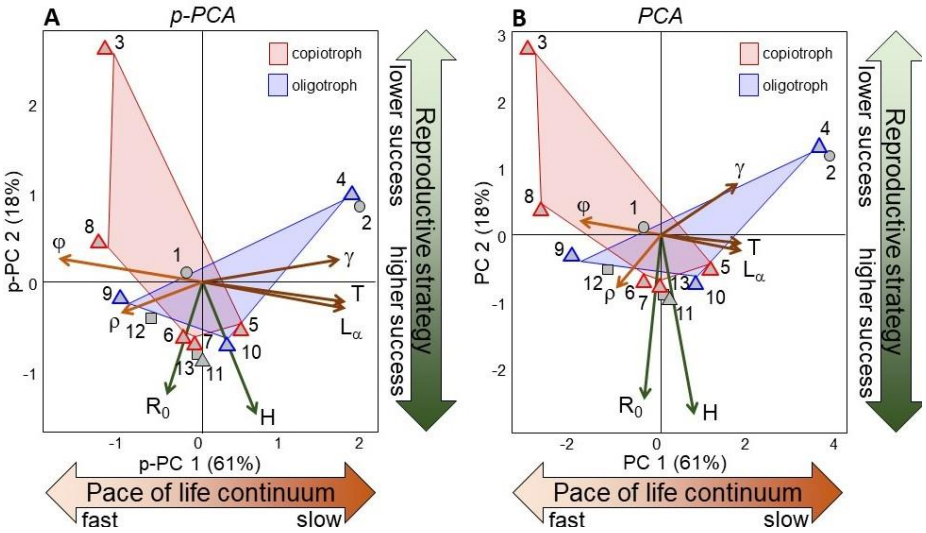

Fig. 2. To characterise life histories, a phylogenetically corrected PCA (p-PCA) (**A**) and a normal PCA (**B**) were performed on generation time *T*, the shape of the survivorship curve *H*, age at maturity L_α, progressive growth γ, retrogressive growth ρ, mean recruitment success φ, and net reproductive rate R_0 (Table 3). Both show the same result. We show the first two PC axes, although the eigenvalue of the third PC axis was also > 1 (following the Kaiser criterion [34]: $\lambda_{axis\ 1} = 4.27$; $\lambda_{axis\ 2} = 1.25$; $\lambda_{axis\ 3} = 1.15$; $\lambda_{axis\ 4} = 0.25$) and the third axis explained 16% of the variation (see further main text). Arrow lengths are proportional to the loadings of each trait onto these two axes. Circles indicate protist or plant, triangles indicate bacteria, and squares indicate fungi. Numbers next to symbols indicate species identity as in Fig. 1 and in Tables 1 and 3. Confirmed classifications of species as copiotroph (red-lined symbols) and oligotroph (blue-lined symbols) (Fig. 1) are indicated in both biplots and the associated convex hulls denote areas of life history strategy space occupied by them.

The two life history traits aligned with p-PC2 represent dimensions of microorganism reproductive strategy not captured by mean recruitment success: both the net reproductive rate (R_0) and the shape of the survivorship curve (*H*) are negatively loaded onto p-PC2: the reproductive strategy axis (Table 2). This means that, as we move from positive to negative scores along p-PC2, microorganisms attain greater lifetime reproductive success while the mortality of older individuals decreases. This time, species classified as copiotrophs and oligotrophs completely overlapped along the reproductive strategy axis (red and blue convex hulls in Fig 2A, respectively).

Table 3. The life history traits generation time T, survivorship curve H, age at sexual maturity L_α, progressive growth γ, retrogressive growth ρ, mean sexual reproduction φ, and net reproductive rate R_0 calculated from DEB-IPMs and analysed using PCAs (Table 2). Species numbers are the same as in Fig. 1.

	Species	Life history trait						
		T	H	L_α	γ	ρ	φ	R_0
1	*Dictyostelium discoideum*	6.11	0.11	5.69	4.29E-05	3.11E-08	0.24	1.69
2	*Chlamydomonas reinhardtii*	73.80	0.27	51.90	1.31E-04	2.35E-06	0.02	0.96
3	*Bacillus subtilis*	2.01	0.02	2.00	3.21E-05	3.49E-06	0.82	1.16
4	*Synechococcus elongatus*	37.54	0.15	31.00	1.73E-04	2.65E-09	0.04	1.32
5	*Mycobacterium smegmatis*	20.65	0.22	18.35	4.72E-05	2.75E-06	0.07	1.49
6	*Pseudomonas aeruginosa*	7.90	0.17	7.63	3.83E-05	8.32E-07	0.18	1.71
7	*Shewanella oneidensis*	10.04	0.18	9.50	3.72E-05	9.17E-07	0.14	1.71
8	*Escherichia coli*	2.27	0.16	2.32	2.13E-05	1.93E-05	0.71	1.20
9	*Caulobacter vibrioides*	2.88	0.21	2.89	2.86E-05	6.99E-06	0.54	1.39
10	*Methylorubrum extorquens*	16.45	0.23	15.20	4.48E-05	2.07E-06	0.09	1.57
11	*Desulfovibrio vulgaris*	8.59	0.34	8.55	5.78E-05	5.40E-06	0.17	1.52
12	*Schizosaccharomyces pombe*	4.24	0.22	4.20	3.87E-05	3.86E-06	0.35	1.50
13	*Saccharomyces cerevisiae*	7.79	0.33	7.81	5.74E-05	5.34E-06	0.18	1.51

Interestingly, p-PC3 is retained [its associated eigenvalue >1 (Fig. 2A)] and explained 16% of the variation. The negative loading of net reproductive rate R_0 onto p-PC3 had an opposite loading for retrogressive growth ρ (Table 2): moving from one end of p-PC3 to the other, microorganisms attain greater (or lower) lifetime reproductive success and tend to shrink less (or more).

Finally, there was a weak phylogenetic signature in the structuring of life history variation (Pagel's λ was close to zero: $\lambda < 0.01$), suggesting a weak role of overall phylogenetic ancestry in life history trait variation, confirmed by traitgrams that showed no strong mapping of a species' place along the pace of life continuum (Fig. 3A) or reproductive strategy axis (Fig. 3B) and its phylogenetic position. We therefore ran a normal PCA, which showed the same results as the p-PCA (Table 3, Fig. 2B).

Discussion

Microorganisms are typically classified as copiotroph or oligotroph but it has been proven difficult to generalise their life history strategies to broad lineages [5]. Here, we assessed if the fast-slow reproductive strategy framework, which has so far only been applied to animals and higher plants [7-9,35], can be applied to microorganisms. We also tested if inferences about life history strategies can be made from patterns in taxonomic composition of microorganisms. Like animals and higher plants, we found that microorganismal life history variation was structured along a fast-slow pace of life continuum and an axis of reproductive strategy [6,9]. But only at the extreme ends of the pace of life continuum was there a match between copiotrophs at the fast end and oligotrophs at the slow

end of the continuum. Our explorative work therefore suggests that the fast-slow reproductive strategy framework can provide a strong predictive framework on the behaviour and activity of microorganism that can to some extent be used alongside the copiotroph-oligotroph dichotomy.

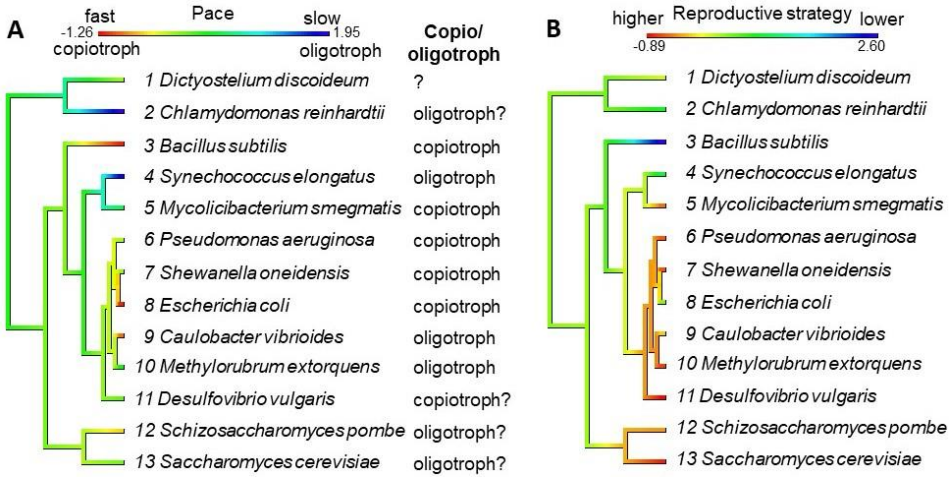

Fig. 3. Traitgrams indicating the relationship between a species' phylogenetic position (as in Fig. 1) and (**A**) its place along the pace of life continuum from fast (negative values in red) to slow (positive values in blue), and (**B**) its place along the reproductive strategy axis from high success (negative values in red) to low success (positive values in blue). Values in (A) are the scores of p-PC1 and values in (B) are the scores of p-PC2 (Fig. 2A). Copiotroph and oligotroph classification was according to [58] (species 1), [5] (species 2-10), [59] (species 11), and [60] (species 12-13) (questions marks indicate suspected classifications).

Like previous life history strategy analyses on animals and higher plants, we found that our findings of microorganismal life history strategies were unaffected by phylogeny. Possibly, plasticity in life history traits (variation of trait values within a species that occurs in response to variability in the environment) is obscuring the phylogenetic signal. For example, microorganisms can switch from fermentation to respiration in response to changes in glucose availability, resulting in great reprogramming of gene expression (e.g., [36]). Also, cell growth in e.g., *S. cerevisiae* and *B. subtilis* depends on food quality [23,37], creating plasticity in growth. When variation among individuals in a species is sufficiently large to approach variation between species, any correlation between species traits and their evolutionary relatedness can be masked. Alternatively, or additionally, the lack of a phylogenetic signal may be due to high life history trait lability (e.g., [38]), or due to weak links between genotype and phenotype evolution mapping as life history traits are typically determined by multiple genes that interact to produce phenotypes in a non-additive or non-linear fashion (e.g [39]). If indeed phylogenetic relationships play a minimal role in determining life history adaptations of microorganisms, environmental filtering stemming from extrinsic factors should be considered as the main process of the evolution of microorganismal life history strategies [1].

The evolution of life history strategies is also shaped by the trade-offs that individual make between investment into survival, growth and reproduction [1]. Firstly, the pace of life continuum in animals and higher plants is underpinned by a trade-off between fast-growing, highly reproductive species and population turnover [7,9]. We also found that the microorganismal pace of life continuum was underpinned by a trade-off between highly reproductive species and population turnover, but the highly reproductive species were associated with low values of progressive growth (γ), and, thus, fast microorganisms were slower, and not faster growers. Perhaps, this is because individual microorganisms grow by enlarging individual cells, whereas macroorganisms, among others, grow by increasing total cell mass [40]. Secondly, a trade-off between current and future reproduction

335 underlies the reproductive strategy axis [41,42]. Highly semelparous species with a single
336 reproductive event in their lifespan and high mortality are ranked at one extreme, and iteroparous
337 species with high spread in reproduction and low mortality on the other [10]. We did find, like
338 animals and higher plants, that the reproductive strategy axis captured variation in net reproductive
339 rate (R_0), but we modelled a semelparous life history strategy for all the microorganisms in our study
340 (as an individual cell dies to produce an offspring and parent cell) [23,43,63]. However, the plant *C.*
341 *reinhardtii*, the fungi *S. pombe* and *S. cerevisiae*, and the protist *D. discoideum* can reproduce
342 sexually [45-47]. Also, when reproducing asexually, *S. cerevisiae* divides via budding, producing a
343 smaller offspring cell and a remaining, larger parent cell. The plant *C. reinhardtii*, in turn, undergoes
344 a multiple-fission cycle, potentially producing up to eight daughter cells [48]. Future endeavours
345 could explore how more complex growth and reproduction patterns affect life history strategy
346 structuring.

347 In conclusion, we identified a pace of life and reproductive strategy axis in microorganisms, albeit for
348 a small number of species. Next steps should at least (i) target more species, including from the field,
349 (ii) systematically control abiotic factors like temperature, and (iii) explore a variety of growth and
350 reproduction patterns. We hope that our first exploration will ignite such research. It could help us
351 understand the diversity of microorganismal phenotypes [49-51], and increase our understanding of
352 how they impact on higher level processes like host phenotype expression [52,53], and human
353 physiology and metabolism [12,13].

354 Author statements

355 Author contributions

356 J.R. contributed to data collection, formal analysis, visualisation, and writing of the first draft. I.M.S.
357 contributed to conceptualisation, supervision and writing of final draft.

358 Conflicts of interest

359 The authors declare that there are no conflicts of interest.

360 Funding information

361 This work received no specific grant from any funding agency.

362 Acknowledgements

363 The authors thank Tom van Dooren for constructive comments on an earlier draft.

364 References

365 1. **Stearns SC.** The Evolution of Life Histories. Oxford University Press, New York; 1992.
366 2. **Koch AL**. Oligotrophs versus copiotrophs. *BioEssays* 2001; 23:657–61.
367 3. **Fierer N, Bradford MA, Jackson RB**. Toward an ecological classification of soil bacteria. *Ecology*
368 2007; 88:1354–1364.
369 4. **Ramin KI, Allison SD**. Bacterial tradeoffs in growth rate and extracellular enzymes. *Front*
370 *Microbiol* 2019; 10: 2956.
371 5. **Stone BWG, Dijkstra P, Finley BK. et al**. Life history strategies among soil bacteria—dichotomy
372 for few, continuum for many. *ISME J.* 2023 17:611-619.
373 6. **Gaillard J-M. et al.** An analysis of demographic tactics in birds and mammals. *Oikos* 1989; 56:
374 59–76.

7. **Paniw M, Ozgul A, Salguero-Gómez R**. Interactive life-history traits predict sensitivity of plants and animals to temporal autocorrelation. *Ecol Lett* 2018; 21: 275–286.
8. **Capdevilla P, Beger M, Blomberg SP, Hereu B, Linares C, Salguero-Gómez R**. Longevity, body dimension and reproductive mode drive differences in aquatic versus terrestrial life history strategies. *Funct Ecol* 2020; 34: 1613–1625.
9. **Salguero-Gómez R, Jones O R, Jongejans E, et al.** Fast–slow continuum and reproductive strategies structure plant life-history variation worldwide. *Proc. Natl. Acad. Sci. USA* 2016; 113: 230–235.
10. **Healy K. et al.** Animal life history is shaped by the pace of life and the distribution of age-specific mortality and reproduction. *Nature Ecol Evol* 2019; 3: 1217-1224.
11. **Evans S. Wallenstein M.** Climate change alters ecological strategies of soil bacteria. *Ecol Lett* 2013; 17: 155-164.
12. **Vrieze A, de Groot PF et al.** Fecal transplant: A safe and sustainable clinical therapy for restoring intestinal microbial balance in human disease? *Best Pract Res Clin Gastroenterol* 2013; 27: 127-137.
13. **Rook G. et al.** Evolution, human-microbe interactions, and life history plasticity. *Lancet* 2017; 390: 521–30.
14. **Meistertzheim A-L et al.** Patterns of bacteria-host associations suggest different ecological strategies between two reef building cold-water coral species. *Deep Sea Res Part I* 2016; 114: 12–22.
15. **Smallegange IM et al.** Mechanistic description of population dynamics using dynamic energy budget theory incorporated into integral projection models. Methods Ecol Evol 2017; 8: 146-154.
16. **Kooijman SALM, Metz JAJ**. On the dynamics of chemically stressed populations: the deduction of population consequences from effects on individuals. *Ecotoxicol Environ Saf* 1984; 8: 254–274.
17. **Margolin W**. Ftsz and the division of prokaryotic cells and organelles. *Nat Rev Mol Cell Biol* 2005; 6: 862–71.
18. **Jager T. et al.** DEBkiss or the quest for the simplest generic model of animal life history. *J Theor Biol* 2013; 328:9-18.
19. **Easterling MR, Ellner SP, Dixon PM**. Size-specific sensitivity: applying a new structured population model. *Ecology* 2000; 81:694–708
20. **Allard C et al**. A size-invariant bud-duration timer enables robustness in yeast cell size control. – *PloS One* 2018; 13: e0209301
21. **Rochaix J-D.** *Chlamydomonas reinhardtii*. In S. Maloy and K. Hughes, editors, Brenner's Encyclopedia of Genetics (Second Edition), pages 521–524. Academic Press, San Diego, second edition; 2013.
22. **Deforet M et al**. Cell-size homeostasis and the incremental rule in a bacterial pathogen. *Biophys J* 2015; 109: 521–528.
23. **Sauls JT et al**. Control of *Bacillus subtilis* replication initiation during physiological transitions and perturbations. *mBio* 2019; 10:e02205-19.
24. **Tanaka M. Yumura S**. A 'dynamic adder model' for cell size homeostasis in *Dictyostelium* cells. *Sci Rep* 2021; 11: 13742.
25. **Fiévet A. et al.** Single-cell analysis of growth and cell division of the anaerobe *Desulfovibrio vulgaris* Hildenborough. *Front Microbiol* 2015; 6: 1378.
26. **R Core Team**. R: A language and environment for statistical computing. R Foundation for Statistical Computing, Vienna, Austria; 2021.
27. **Romeijn J, Smallegange IM**. Exploring how the fast-slow pace of life continuum and cell size structure microorganism life history variation. Figshare. Online resource. 2021; https://doi.org/10.6084/m9.figshare.16831543.v2

28. **Revell LJ.** phytools: An R package for phylogenetic comparative biology (and other things). - Methods Ecol Evol 2012; 3: 217–223.
29. **Freckleton RP et al.** Phylogenetic analysis and comparative data: a test and review of evidence. *Am Nat* 2012; 160: 712–726.
30. **Haywood-Farmer E. Otto SP.** The evolution of genomic base composition in bacteria. *Evolution* 2003; 57: 1783-1792.
31. **Münkemüller T, Lavergne S, Bzeznik B, Dray S, Jombart T, Schiffers K, Thuiller W.** How to measure and test phylogenetic signal. *Methods Ecol Evol* 2012; 3: 743– 756.
32. **Hansen TF**. Stabilizing selection and the comparative analysis of adaptation. *Evolution* 1997; 51:1341–1351.
33. **Martins EP. Hansen TF.** Phylogenies and the comparative method: a general approach to incorporating phylogenetic information into the analysis of interspecific data. *Am Nat* 1997; 149:646–667.
34. **Legendre P. Legendre L.** Numerical Ecology, 3rd ed. Elsevier, London, pp. 1006; 2012.
35. **Smallegange IM. et al.** Unusually paced life history strategies of marine megafauna drive atypical sensitivities to environmental variability. *Frontiers Mar Sci* 2020; 7:597492.
36. **Roberts GG. Hudson AP**. Transcriptome profiling of Saccharomyces cerevisiae during a transition from fermentative to glycerol-based respiratory growth reveals extensive metabolic and structural remodeling. *Mol Genet Genomics* 2006; 276: 170–186
37. **Ferrezuelo F. et al**. The critical size is set at a single-cell level by growth rate to attain homeostasis and adaptation. *Nature Comm* 2012; 3: 1012.
38. **Savage JA, Cavender-Bares J.** Habitat specialization and the role of trait lability in structuring diverse willow (genus *Salix*) communities. *Ecology* 2012; 93: S138–S150.
39. **Zörgö E, Gjuvsland A, Cubillos FA, Louis EJ, Liti G, Blomberg A, Omholt SW, Warringer J**. Life history shapes trait heredity by accumulation of loss-of-function alleles in Yeast. *Mol Biol Evol* 2012; 29: 1781-1789.
40. **Conlon I, Raff M**. Size control in animal development. *Cell* 1999; 96: 235-244.
41. **Charnov EL, Schaffer WM**. Life-history consequences of natural selection: Cole's result revisited. *Am Nat* 1973; 107:791–793.
42. **Shaw AK, Levin SA**. The evolution of intermittent breeding. *J Math Biol* 2013; 66:685–703.
43. **Campos M. et al**. A constant size extension drives bacterial cell size homeostasis. *Cell* 2014; 159:1433-1446.
44. **Taheri-Araghi S. et al**. Cell-size control and homeostasis in bacteria. Curr Biol 2015; 25:385-391.
45. **Nielsen O.** Mating-Type Control and Differentiation. In: Egel R. (eds) The Molecular Biology of *Schizosaccharomyces pombe*. Springer, Berlin, Heidelberg; 2004.
46. **Urushihara H. Muramoto T**. Genes involved in *Dictyostelium discoideum* sexual reproduction. *Europ J Cell Biol* 2006; 85: 961–968.
47. **Wallen R. Perlin M.** An overview of the function and maintenance of sexual reproduction in dikaryotic fungi. Frontiers Microbiol. 2018; 9: 503.
48. **Cross F. Umen J.** The chlamydomonas cell cycle. *Plant J* 2015; 82: 370-392.
49. **Keymer JE**. Bacterial metapopulations in nanofabricated landscapes. *Proc Natl Acad Sci USA* 2006; 103: 17290-17295.
50. **Santillan E. et al**. Trait-based life-history strategies explain succession scenario for complex bacterial communities under varying disturbance. *Environ Microbiol* 2019; 21: 3751-3764.
51. **Kiørboe T. Thomas MK**. Heterotrophic eukaryotes show a slow-fast continuum, not a gleaner–exploiter trade-off. *Proc Natl Acad Sci USA* 2020; 117: 24893-24899.
52. **Kopecky J. et al**. The effect of antibiotics on associated bacterial community of stored product mites. *PLoS ONE* 2014; 9: e112919
53. **Zindel R. et al**. The role of the bacterial community in the nutritional ecology of the bulb mite *Rhizoglyphus robini* (Acari: Astignmata: Acaridae). *FASEB J* 2017; 27: 1488-1497.

54. **Michonneau F.** rotl, an R package to interact with the Open Tree of Life data. *PeerJ Preprints* 2016; 4:e1471v3.
55. **Hinchliff CE et al.** Synthesis of phylogeny and taxonomy into a comprehensive tree of life. *Proc Natl Acad Sci USA* 2015; 112: 201423041.
56. **Chamberlain S. Szocs E.** taxize - taxonomic search and retrieval in R. *F1000Research* 2013; 2: 191.
57. **Paradis E et al.** APE: Analyses of phylogenetics and evolution in R language. *Bioinformatics* 2004; 20: 289–290.
58. **Layboum-Parry J, Marchant HJ, Brown P.** The plankton of a large oligotrophic freshwater Antarctic lake. *Journal of Plankton Research* 1991; 13: 1137–1149.
59. **Orellana R, Arancibia A, Badilla L, Acosta J, Arancibia G, Escar R, Ferrada G, Seeger M.** Ecophysiological features shape the distribution of prophages and CRISPR in sulfate reducing prokaryotes. *Microorganisms* 2021; 9: 931.
60. **Ho A,Di Lonardo DP, Bodelier PLE**. Revisiting life strategy concepts in environmental microbial ecology. *FEMS Microbiology Ecology* 2023; 93: fix006.
61. **Buchwald P, Sveiczer A.** The time-profile of cell growth in fission yeast: Model selection criteria favoring bilinear models over exponential ones. - *Theor Biol Med Mod* 2006; 3:16.
62. **Nobs J-B, Maerkl S.** Long-term single cell analysis of *S. pombe* on a microfluidic microchemostat array. *PloS ONE* 2014; 9: e93466.
63. **Sauls JT. et al**. Adder and a coarse-grained approach to cell size homeostasis in bacteria. Curr Opin. *Cell Biol* 2016; 38: 38–44.
64. **Priestman M. et al.** Mycobacteria modify their cell size control under sub-optimal carbon sources. *Front Cell Dev Biol* 2017; 5:64.
65. **Aldridge B. et al**. Asymmetry and aging of mycobacterial cells lead to variable growth and antibiotic susceptibility. *Science* 2011; 335: 100–104.
66. **Nieto C. et al.** Unification of cell division control strategies through continuous rate models. *Phys Rev E* 2020; 101: 022401.
67. **Zheng H. et al.** Interrogating the *Escherichia coli* cell cycle by cell dimension perturbations. *Proc Natl Acad Sci USA* 2016; 113: 15000-15005.
68. **Steel C. et al.** Single live cell imaging of chromosomes in chloramphenicol-induced filamentous *Pseudomonas aeruginosa*. *Biochemistry* 2004; 43: 175–182.
69. **Lee CK. et al.** Evolution of Cell Size Homeostasis and Growth Rate Diversity during Initial Surface Colonization of *Shewanella oneidensis*. *ACS Nano* 2016; 10:9183-9192.
70. **Banerjee S. et al**. Biphasic growth dynamics control cell division in *Caulobacter crescentus*. *Nature Microbiology* 2017; 2: 17116.
71. **Beaufay F et al.** A NAD-dependent glutamate dehydrogenase coordinates metabolism with cell division in *Caulobacter crescentus*. *The EMBO journal 2015*; 34: 1786-1800.
72. **Martins BMC. et al**. Cell size control driven by the circadian clock and environment in cyanobacteria. *Proc Natl Acad Sci USA* 2018; 115: E11415-E1142.
73. **Vitova M. et al.** *Chlamydomonas reinhardtii*: Duration of its cell cycle and phases at growth rates affected by light intensity. *Planta* 2010; 233: 75–86.
74. **Strovas T. et al.** Cell-to-cell heterogeneity in growth rate and gene expression in *Methylobacterium extorquens* AM1. *J Bacteriology* 2007; 189: 7127–7133.
75. **Caswell H.** Matrix Population Models. Sunderland, MA: Sinauer Associates; 2001.
76. **Caswell H.** Sensitivity analysis: Matrix Methods in Demography and Ecology. Demographic Research Methods. Springer Open; 2018.
77. **Tuljapurkar S, Gaillard JM, Coulson T.** From stochastic environments to life histories and back. *Phil Trans Roy Soc B* 2009; 364: 1499-1509.
78. **Keyfitz N, Caswell H**. Applied mathematical demography. Springer, third edition edn; 2005.
79. **Sveiczer A. et al**. The size control of fission yeast revisited. *J Cell Sci* 1997; 109: 2947–2957.